

# Location of the Alkali Metal Ion in Gas-Phase Peptide Complexes

Lynn M. Teesch,<sup>†</sup> Ronald C. Orlando,<sup>‡</sup> and Jeanette Adams<sup>\*†</sup>

Contribution from the Department of Chemistry, Emory University, Atlanta, Georgia 30322, and the Structural Biochemistry Center, Department of Chemistry, University of Maryland Baltimore County, Baltimore, Maryland 21228. Received October 19, 1990.

Revised Manuscript Received January 23, 1991

**Abstract:** Collision-induced decompositions of gas-phase  $(M + \text{Cat})^+$  complexes between 55 peptides and  $\text{Li}^+$ ,  $\text{Na}^+$ ,  $\text{K}^+$ ,  $\text{Rb}^+$ , and  $\text{Cs}^+$  were studied either as first field-free region reactions by using B/E scans or as third field-free region reactions by using MS-MS. Results from these and MS-MS-MS experiments provide evidence that  $(b_{n-m} + \text{Cat} + \text{OH})^+$  product ions arise from complexes that contain the metal ion bonded on the N-terminal side of the reaction site; the intramolecular nucleophilic reaction first proposed by Westmore and co-workers explains their formation. Furthermore, formation of  $(b_{n-m} + \text{Cat} + \text{H})^+$  product ions can be understood in terms of a 1,2-elimination that occurs from  $(M + \text{Cat})^+$  complexes that likewise contain the metal ion bonded toward the N-terminus. Changes in metastable ion vs CID spectra with changes in side-chain structure support decompositions of complexes in which the metal ion is multidentate bonded to carbonyl oxygen atoms in the peptide backbone and to chelating side chains. All our results indicate that structures of gas-phase  $(M + \text{Cat})^+$  complexes between peptides and alkali metal ions do not reflect solution-phase binding to a peptide zwitterion but more closely reflect the types of intramolecular, multisite binding interactions that might occur in less hydrophilic interiors of proteins.

The intrinsic, gas-phase chemistry of interactions between metal(I) ions and monofunctional organic ligands has been of interest to both experimentalists and theoreticians. The gas-phase equilibrium binding strengths between alkali,<sup>1</sup> and other metal(I),<sup>2</sup> ions and simple organic ligands have provided important experimental data from which theoretical molecular orbital calculations have been evaluated.<sup>3</sup> Furthermore, analytical applications of such metal-ligand interactions have resulted in new approaches for mass spectrometric structure determination of simple biological molecules.<sup>4</sup> These applications have basis in the early work of Röllgen and co-workers,<sup>5</sup> who first showed that collision-induced decompositions (CID) of  $(M + \text{Cat})^+$  ions, in which M = molecule and Cat = alkali metal ion, can be significantly different from CID of analogous protonated  $(M + \text{H})^+$  ions.

The gas-phase chemistry, and CID, of complexes between metal(I) ions and more complicated polyfunctional biological ligands such as peptides has also become of interest. Cody, Amster, and McLafferty<sup>6</sup> first demonstrated that laser-desorbed  $(M + \text{K})^+$  complexes of gramicidin D and S fragment by CID to give valuable structural information. Subsequently, other researchers<sup>7-11</sup> have sought to understand the gas-phase reactions and to use the fragmentation chemistry to elucidate the metal ion binding interactions in the peptide-alkali ion  $(M + \text{Cat})^+$  complexes. Russell and co-workers<sup>7</sup> used relative product ion abundances to draw hypotheses regarding the preferential alkali ion binding sites; they concluded that the metal ion either is bonded intramolecularly to amide nitrogens and to the amino terminus, or is bonded to amide nitrogens and side-chain substituents. Westmore and co-workers<sup>8</sup> performed other experiments and concluded instead that the alkali metal ion in the gas-phase complexes is intramolecularly bonded to amide carbonyl oxygens. Renner and Spiteller,<sup>9</sup> and more extensively Gross and co-workers,<sup>10</sup> provided alternative explanations for the chemistry in which the alkali ion is bonded instead to the deprotonated (zwitterionic) carboxylate terminus of the peptide. Leary and co-workers,<sup>11</sup> from both experimental and theoretical data, suggested that the gas-phase fragmentations reflect a combination of some of the above ideas, with emphasis<sup>11b</sup> on complexation of the metal ion to carbonyl oxygens.

In another recent investigation, we<sup>12</sup> presented new information regarding the location of the alkali metal ion in gas-phase peptide  $(M + \text{Cat})^+$  complexes. Our proposed mechanisms of fragmentation provided evidence that formation of N-terminal  $(a_{n-m} +$

$\text{Cat} - \text{H})^+$  and C-terminal  $(y_{n-m} + \text{Cat} + \text{H})^+$  product ions, and another special product ion, involves complexes in which the metal ion would be bonded, for instance, to a basic amide oxygen and not to a deprotonated C-terminal carboxylate. Consequently, our data indicated that the gas-phase chemistry more closely reflects intrinsic interactions between metal ions and peptides and not solution-phase binding to a zwitterionic carboxylate. We<sup>13</sup> drew similar conclusions from mechanistic data regarding the gas-phase chemistry of  $(M + \text{Cat}^{2+} - \text{H})^+$  complexes between peptides and alkaline earth metal ions.

Here we present more evidence regarding the location of the alkali metal ion in gas-phase peptide  $(M + \text{Cat})^+$  complexes. We

- (1) (a) Džidić, I.; Kebarle, P. J. *Phys. Chem.* **1970**, *74*, 1466-1476. (b) Staley, R. H.; Beauchamp, J. L. *J. Am. Chem. Soc.* **1975**, *97*, 5920-5921. (c) Castleman, A. W., Jr.; Holland, P. M.; Lindsay, D. M.; Peterson, K. I. *J. Am. Chem. Soc.* **1978**, *100*, 6039-6045. (d) Taft, R. W.; Anvia, F.; Gal, J.-F.; Walsh, S.; Capon, M.; Holmes, M. C.; Hosn, K.; Oloumi, G.; Vasanwala, R.; Yazdani, S. *Pure Appl. Chem.* **1990**, *62*, 17-23.
- (2) (a) Uppal, J. S.; Staley, R. H. *J. Am. Chem. Soc.* **1982**, *104*, 1229-1234. (b) Uppal, J. S.; Staley, R. H. *J. Am. Chem. Soc.* **1982**, *104*, 1235-1238. (c) Uppal, J. S.; Staley, R. H. *J. Am. Chem. Soc.* **1982**, *104*, 1238-1243.
- (3) (a) Woodin, R. L.; Houle, F. A.; Goddard, W. A., III *Chem. Phys.* **1976**, *14*, 461-468. (b) Hinton, J. F.; Beeler, A.; Harpool, D.; Briggs, R. W.; Pullman, A. *Chem. Phys. Lett.* **1977**, *47*, 411-415. (c) Kollman, P.; Rothenberg, S. *J. Am. Chem. Soc.* **1977**, *99*, 1333-1342. (d) Smith, S. F.; Chandrasekhar, J.; Jorgensen, W. L. *J. Phys. Chem.* **1982**, *86*, 3308-3318. (e) Del Bene, J. E. *J. Comput. Chem.* **1986**, *7*, 259-264.
- (4) (a) A recent review that discusses charge-remote fragmentations of biological molecules that are cationized with alkali metal ions is: Adams, J. *Mass Spectrom. Rev.* **1990**, *9*, 141-186. (b) Contado, M. J.; Adams, J.; Gross, M. L. *Adv. Mass Spectrom.* **1989**, *11B*, 1034-1035. (c) Crockett, J. S.; Gross, M. L.; Christie, W. W.; Holman, R. T. *J. Am. Soc. Mass Spectrom.* **1990**, *1*, 183-191. (d) Contado, M. J.; Adams, J. *Anal. Chim. Acta.* In press.
- (5) Röllgen, F. W. K.; Borchers, F.; Giessmann, U.; Levsen, K. *Org. Mass Spectrom.* **1977**, *12*, 541-543.
- (6) Cody, R. B.; Amster, I. J.; McLafferty, F. W. *Proc. Natl. Acad. Sci., U.S.A.* **1985**, *82*, 6367-6370.
- (7) (a) Mallis, L. M.; Russell, D. H. *Anal. Chem.* **1986**, *58*, 1076-1080. (b) Russell, D. H. *Mass Spectrom. Rev.* **1986**, *5*, 167-189. (c) Russell, D. H.; McGlohon, E. S.; Mallis, L. M. *Anal. Chem.* **1988**, *60*, 1818-1824. (8) Tang, X.; Ens, W.; Standing, K. G.; Westmore, J. B. *Anal. Chem.* **1988**, *60*, 1791-1799.
- (9) Renner, D.; Spiteller, G. *Biomed. Environ. Mass Spectrom.* **1988**, *15*, 75-77.
- (10) (a) Grese, R. P.; Cerny, R. L.; Gross, M. L. *J. Am. Chem. Soc.* **1989**, *111*, 2835-2842. (b) Grese, R. P.; Gross, M. L. *J. Am. Chem. Soc.* **1990**, *112*, 5098-5104.
- (11) (a) Leary, J. A.; Williams, T. D.; Bott, G. *Rapid Commun. Mass Spectrom.* **1989**, *3*, 192-196. (b) Leary, J. A.; Zhou, Z.; Ogdan, S. A.; Williams, T. D. *J. Am. Soc. Mass Spectrom.*, **1990**, *1*, 473-480.
- (12) Teesch, L. M.; Adams, J. *J. Am. Chem. Soc.* **1991**, *113*, 812-820.
- (13) Teesch, L. M.; Adams, J. *J. Am. Chem. Soc.* **1990**, *112*, 4110-4120.

<sup>†</sup> Emory University.

<sup>‡</sup> University of Maryland Baltimore County.

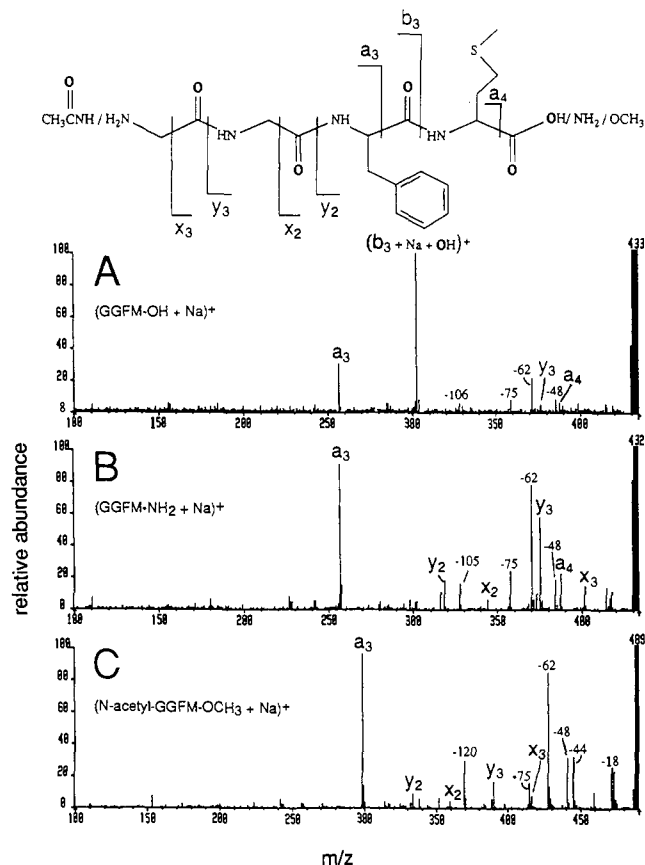


**Figure 1.** CID spectra of  $(M + Na)^+$  complexes of (A) Gly-Gly-Phe-Met acid, (B) Gly-Gly-Phe-Met amide, and (C) *N*-acetyl-Gly-Gly-Phe-Met ester acquired by using B/E scans and the VG 70-S (at Emory). Ions labeled  $a_{n-m}$ ,  $x_{n-m}$ , and  $y_{n-m}$  are  $(a_{n-m} + Na - H)^+$ , and  $(y_{n-m} + Na + H)^+$  ions, respectively.

particularly address formation of the abundant N-terminal  $(b_{n-1} + Cat + OH)^+$  product ion. This ion is of major interest because conflicting mechanisms for its formation have been reported: Westmore and co-workers<sup>8</sup> proposed that it arises from an intramolecular nucleophilic displacement reaction via an attacking  $-COOH$  group, whereas Renner and Spiteller,<sup>9</sup> Gross and co-workers,<sup>10</sup> and Leary et al.<sup>11</sup> instead proposed that the nucleophile is an attacking  $-COO^-$  group. We also address formation of  $(b_{n-m} + Cat - H)^+$  ions and discuss changes in fragment ion abundances in metastable ion vs CID spectra in relation to effects of side-chain structure on the kinetics of the different fragmentation reactions.

## Results

Metastable ion and collision-induced decompositions (CID) of gas-phase  $(M + Cat)^+$  complexes between 55 peptides and  $Li^+$ ,  $Na^+$ ,  $K^+$ ,  $Rb^+$ , and  $Cs^+$  were studied either as first field-free region reactions by using B/E scans and a two-sector, forward geometry mass spectrometer (at Emory) or as third field-free region reactions by using a tandem, four-sector mass spectrometer (at UMBC). Fast atom bombardment (FAB) was used to form the ions from a mixture of the peptide, a FAB matrix, and an alkali iodide. The peptides ranged from di- to heptapeptides, and some contained either a C-terminal carboxylate, amide, methyl ester, or alcohol group. Others contained an N-terminal benzoyl or *tert*-butyloxycarbonyl (*t*-BOC) group. Some had been *N*-acetylated, unless previously *N*-benzoylated, and then *N,O*-per-methylated.

We previously<sup>12</sup> showed several examples of CID spectra of  $(M + Cat)^+$  complexes between different alkali metal ions and several of the different types of peptides. To summarize, as long as  $Cat = Li^+$  or  $Na^+$ , the most abundant product ion in both metastable ion and CID spectra of peptide C-terminal carboxylates is usually the  $(b_{n-1} + Cat + OH)^+$  ion (Figure 1A). The absolute abundance of this ion generally decreases with increasing size of

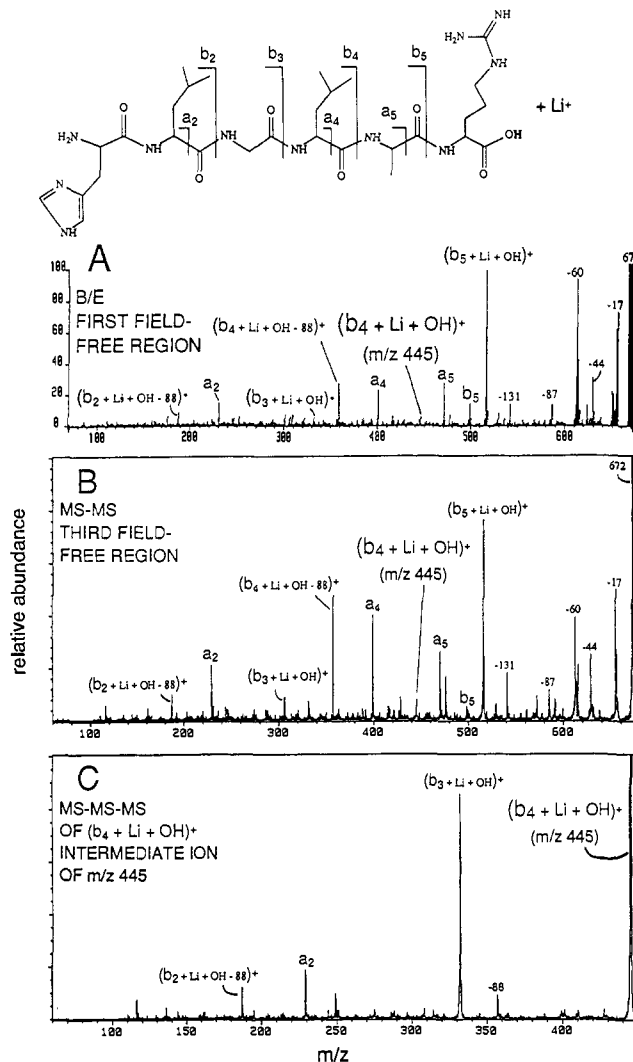
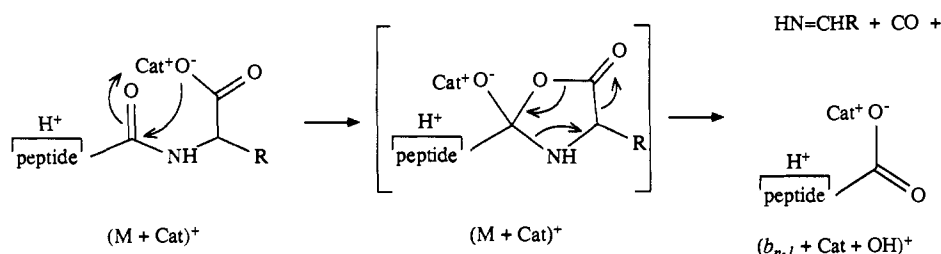


**Figure 2.** CID spectra of  $(M + Li)^+$  complexes of His-Leu-Gly-Leu-Ala-Arg from (A) the first field-free region of VG 70-S, 7-keV Ar for FAB, 8-kV accelerating voltage, 50% beam reduction, He collision gas (at Emory), and (B) the third field-free region of JEOL HX110/HX110, 6-keV Xe for FAB, 10-kV accelerating voltage, 70% beam reduction, He collision gas (at UMBC). The spectrum in (C) is a MS-MS-MS spectrum of first-generation  $(b_4 + Li + OH)^+$  intermediate ions of  $m/z$  445, which were formed in the first field-free region, energy and mass selected, and then collisionally dissociated in the third field-free region of the JEOL HX110/HX100 (same conditions as for spectrum B). Ions labeled  $a_{n-m}$ ,  $b_{n-m}$ , and  $y_{n-m}$  are  $(a_{n-m} + Li - H)^+$ ,  $(b_{n-m} + Li - H)^+$ , and  $(y_{n-m} + Li + H)^+$  ions, respectively.

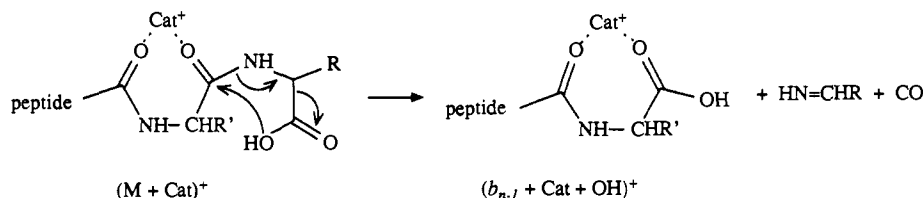
alkali metal ion, to the point that it is virtually undetected in spectra of  $(M + Cs)^+$  complexes (see spectra in ref 12). As the  $(b_{n-1} + Cat + OH)^+$  product ion decreases in absolute abundance, other product ions such as the  $(a_{n-1} + Cat - H)^+$  ion (" $a_3$ " in Figure 1) and ions from cleavages of side chains generally increase in absolute abundances. Furthermore, the  $(b_{n-1} + Cat + OH)^+$  product ion, as first reported by Gross and co-workers<sup>10a</sup> and later by us,<sup>12</sup> is not detected in spectra of either C-terminal amides (Figure 1B) or esters (Figure 1C), although the absolute abundances of other product ions generally increase. These other product ions are primarily N-terminal  $(a_{n-m} + Cat - H)^+$  and C-terminal  $(y_{n-m} + Cat + H)^+$  ions (" $y_3$ " and others in Figure 1).

Each spectrum in Figure 1 also shows a product ion from a loss of either 106, 105 u, or 120 u (Figure 1, A-C, respectively) that arises from a special rearrangement reaction<sup>12</sup> to be discussed further below. The reaction gives loss of 131 u for peptides that contain C-terminal Arg (Figure 2A,B). For C-terminal Leu, the elimination reaction gives loss of 88 u, and the CID spectrum of  $(M + Li)^+$  complexes of His-Leu-Gly-Leu-Ala-Arg (HLGLAR,

Scheme I



Scheme II



Scheme III

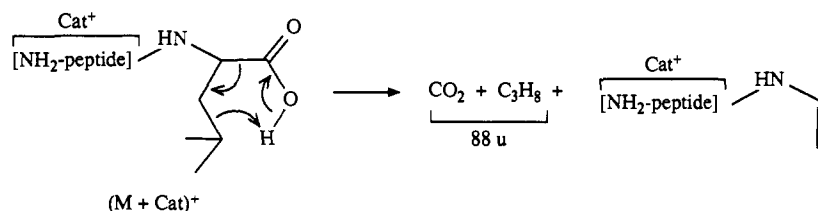


Figure 2A,B) shows two  $(b_{n-m} + \text{Li} + \text{OH} - 88)^+$  ions. The origin and identity of the  $(b_4 + \text{Li} + \text{OH} - 88)^+$  product ion was confirmed from an MS-MS-MS ( $\text{MS}^3$ ) experiment performed by using the tandem, four-sector mass spectrometer. Here, the  $(M + \text{Li})^+$  complexes undergo CID in the first field-free region to give the first-generation  $(b_4 + \text{Li} + \text{OH})^+$  product ions of  $m/z$  445 shown in Figure 2A,B. These "intermediate" ions are subsequently energy and mass selected, and then they undergo CID in the third field-free region to lose 88 u as shown in Figure 2C (see Experimental Section for details).

### Discussion

**Formation of  $(b_{n-1} + \text{Cat} + \text{OH})^+$  Product Ions.** As mentioned above, the mechanism for formation of the  $(b_{n-1} + \text{Cat} + \text{OH})^+$  ions has been debated by several research groups. The importance of the mechanism involves the location of the alkali metal ion, which dictates whether bonding in gas-phase peptide  $(M + \text{Cat})^+$  complexes more closely reflects solution- or gas-phase (intrinsic) chemistry. Russell and co-workers<sup>7</sup> originally described this product ion as a *c*-sequence ion. We now know, however, that  $(M + \text{Cat}^{2+} - \text{H})^+$  complexes between *alkaline earth* ions and peptides *do* fragment to give abundant *c*-sequence ions,<sup>13</sup> but we have never observed  $(M + \text{Cat})^+$  complexes between *alkali* ions and peptides to give *c* ions.<sup>12</sup>

Renner and Spittler<sup>9</sup> correctly reported the identity of the  $(b_{n-1} + \text{Cat} + \text{OH})^+$  product ions and first proposed that the mechanism for their formation involves an intramolecular nucleophilic attack by a deprotonated and cationized C-terminal carboxylate anion (Scheme I). Their mechanism requires the alkali metal ion to be bonded to a zwitterionic peptide in the type of metal ion interaction that would be prevalent in the solution phase. Conversely, Westmore and co-workers<sup>8</sup> offered an alternative mechanism (Scheme II) in which the attacking nucleophile instead is a neutral carboxylate and the alkali metal ion is instead located on the N-terminal side of the reaction site. Their mechanism instead requires the alkali metal ion to be bonded to intrinsically basic site(s)<sup>1b,3b,c</sup> in a neutral peptide molecule.

Grese, Cerny, and Gross<sup>10a</sup> argued in favor of Renner and Spittler's mechanism (Scheme I) because, as shown here in Figure 1, C-terminal esters and amides do not fragment to give detectable

ions that would be analogous to the  $(b_{n-1} + \text{Cat} + \text{OH})^+$  product ions that arise from C-terminal acids. They also argued that if the Westmore mechanism (Scheme II) were correct, migration of methoxide in C-terminal methyl esters should still occur to give  $(b_{n-1} + \text{Cat} + \text{OCH}_3)^+$  ions. Gross and co-workers<sup>10</sup> confirmed from MS-MS-MS ( $\text{MS}^3$ ) experiments that the  $(b_{n-1} + \text{Cat} + \text{OH})^+$  product ion is indeed a new cationized peptide derived from the original peptide less the C-terminal amino acid  $-\text{NHCHR}-\text{CO}$  group. They also used this information to support the mechanism in Scheme I.

Although the product neutrals are the same in both Schemes I and II, the precursor and product ions differ structurally in the location of the alkali metal ion. Thus, one way to determine experimentally which of the two mechanisms is correct is to elucidate the location of the metal cation in the  $(b_{n-m} + \text{Cat} + \text{OH})^+$  product ion; we do this by using information both from  $\text{MS}^3$  experiments and from other mechanisms of fragmentation. For example, the  $\text{MS}^3$  spectrum in Figure 2C shows that the  $(b_4 + \text{Li} + \text{OH})^+$  intermediate ions undergo decomposition to give the  $(a_2 + \text{Li} - \text{H})^+$  ions (" $a_2$ " in Figure 2C). We<sup>12</sup> and Leary and co-workers<sup>11b</sup> presented evidence previously that the mechanism for formation of  $(a_{n-m} + \text{Cat} - \text{H})^+$  ions involves precursor complexes that contain the alkali metal ion bonded toward the N-terminus of the peptide and not to a deprotonated C-terminal carboxylate. Indeed the spectrum in Figure 1C of a C-terminal ester shows that formation of  $(a_{n-m} + \text{Cat} - \text{H})^+$  ions does not involve precursor species that contain a deprotonated and cationized C-terminal carboxylate. These data imply that the  $(b_4 + \text{Li} + \text{OH})^+$  product ion does not have the structure shown in Scheme I.

Stronger evidence regarding the location of the alkali metal ion in  $(b_{n-m} + \text{Cat} + \text{OH})^+$  product ions involves loss of 88 u from the  $(b_4 + \text{Li} + \text{OH})^+$  ion (Figure 2C). We previously<sup>12</sup> presented evidence for a rearrangement reaction that gives loss of 88 u as  $\text{CO}_2$  and  $\text{C}_3\text{H}_8$  from C-terminal Leu (Scheme III). Other peptides also undergo similar reactions, and product ions from several of these are revealed in Figures 1 and 2. For example, the reaction in Scheme III involves concomitant loss of 106 u as  $(\text{CH}_3)_2\text{S}$  and  $\text{CO}_2$  for C-terminal Met-acid (Figure 1A); 105 u as  $(\text{CH}_3)_2\text{S}$  and  $\text{CONH}$  for Met-amide (Figure 1B); and 120 u

as  $\text{CH}_3\text{CH}_2\text{SCH}_3$  and  $\text{CO}_2$  for Met-ester (Figure 1C). The elimination for C-terminal Arg gives loss of 131 u as  $\text{CO}_2$  and  $\text{C}_3\text{H}_7\text{N}_3$  (Figure 2, A and B). In addition, the reaction in Scheme III cannot occur for C-terminal Gly, Ala, Phe, or His, and indeed analogous product ions from these amino acids are never observed.<sup>12</sup> This is why the spectra in Figure 2 do not show side-chain losses from the  $(b_5 + \text{Li} + \text{OH})^+$  and  $(b_3 + \text{Li} + \text{OH})^+$  ions.

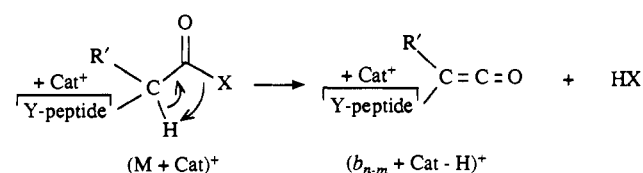
From the structure shown in Figure 2, previous work by Gross and co-workers,<sup>10</sup> and other MS<sup>3</sup> experiments performed here, we know that the  $(b_4 + \text{Li} + \text{OH})^+$  product ions (Figure 2) would have the structure of  $(\text{HLGL} + \text{Li})^+$ . For example, our MS<sup>3</sup> experiments show that the  $(b_5 + \text{Na} + \text{OH})^+$  product ions from  $(\text{M} + \text{Na})^+$  complexes of YGGFLK give the same CID spectrum as  $(\text{M} + \text{Na})^+$  complexes of YGGFL; the  $(b_2 + \text{Na} + \text{OH})^+$  ions from complexes of ALG give the same spectrum as  $(\text{M} + \text{Na})^+$  complexes of Al. Consequently, loss of 88 u from the  $(b_4 + \text{Li} + \text{OH})^+$  ions can be understood entirely from loss of the side chain of the now C-terminal Leu via the reaction in Scheme III. Although there is no detectable  $(b_2 + \text{Li} + \text{OH})^+$  product ions in spectra in Figure 2, these ions would have the structure of  $(\text{HL} + \text{Li})^+$ , and formation of the  $(b_2 + \text{Li} + \text{OH} - 88)^+$  ion can likewise be understood from a similar loss of the now C-terminal Leu side chain. Other  $(\text{M} + \text{Cat})^+$  complexes also fragment to give  $(b_{n-m} + \text{Cat} + \text{OH})^+$  ions that then decompose via the reaction in Scheme III. They include complexes of ALG, GLF, MLF, and GLY, which all fragment to give  $(b_2 + \text{Cat} + \text{OH} - 88)^+$  ions; FLEEL and FLEEI, which give  $(b_4 + \text{Cat} + \text{OH} - 104)^+$  and  $(b_3 + \text{Cat} + \text{OH} - 104)^+$  ions; and YGGFLK, which gives  $(b_3 + \text{Cat} + \text{OH} - 88)^+$  ions. (The reaction sequences were verified from MS<sup>3</sup> experiments in the cases of YGGFLK and ALG.)

The mechanism in Scheme III specifically requires the precursor peptide-metal ion complexes to contain the alkali metal ion bonded on the N-terminal side of the site of reaction. It should be clear that for this reaction to occur for peptide carboxylates, the alkali metal ion cannot be bonded to a deprotonated (zwitterionic) C-terminal carboxylate. Therefore, the  $(b_{n-m} + \text{Cat} + \text{OH})^+$  product ions cannot have the structure shown in Scheme I because then they could not subsequently fragment to give, for example, loss of 88 u in Figure 2. These data indicate that the  $(b_{n-m} + \text{Cat} + \text{OH})^+$  product ions must contain a neutral C-terminal carboxylate, and the alkali metal ion must be bonded to the peptide somewhere toward the N-terminus. These experimental results mean that the mechanism in Scheme I does not, but the mechanism in Scheme II does, describe formation of  $(b_{n-m} + \text{Cat} + \text{OH})^+$  product ions.

The mechanism in Scheme II, in which the metal ion is intramolecularly bonded on the N-terminal side of the bond being cleaved, also reconciles fundamental difficulties inherent with the alternative mechanism in Scheme I. That is, the mechanism in Scheme I is not in accord with the intrinsic bond strengths and preferential geometries of complexes formed between the formate anion and alkali metal ions.<sup>14</sup> Theoretical calculations indicate that gas-phase bonding in  $\text{HCO}_2^-\text{Li}^+$  would preferentially involve a resonance-stabilized bridged structure in which the O-Li-O bond strengths would be  $\sim 171 \text{ kcal mol}^{-1}$ .<sup>14a</sup> In addition, the bridged structure would be favored over a nonbridged structure, such as shown in Scheme I, by  $\sim 18 \text{ kcal mol}^{-1}$ . Recent semiempirical calculations by Leary et al.<sup>11b</sup> also indicate that complexes that contain the alkali ion intramolecularly bonded to amide oxygens would be  $\sim 70 \text{ kcal mol}^{-1}$  lower in energy than a complex that contains the metal ion bonded to a deprotonated C-terminal carboxylate in a bridged configuration.

An important question arises as to whether FAB-desorbed  $(\text{M} + \text{Li})^+$  ions, or intermediate  $(b_{n-1} + \text{Li} + \text{OH})^+$  ions formed by CID, undergo in-flight isomerization. For example, in a MS<sup>3</sup> experiment, does the structure of the  $(b_{n-1} + \text{Li} + \text{OH})^+$  intermediate ion that is probed in the second CID step actually reflect

Scheme IV



its structure as formed by the first CID step? This question cannot be either completely or unambiguously answered because we do not have detailed knowledge of the potential energy surface for this complex system. With basis in the relative energies described in the preceding paragraph, however, the majority of ions that are fragmenting to give  $(b_{n-m} + \text{Li} + \text{OH})^+$  ions should have the original structure shown in Scheme II, and isomerization should be of minimal importance. That is, the system prefers to stay in the conformation with the highest density of states, which is the one of lowest potential energy, represented by the structure in Scheme II.

The observation that neither amides nor esters (Figure 1, B and C, respectively) react via Scheme II is in complete accord with their known abilities to undergo intramolecular nucleophilic attack, at least in the solution phase. The reaction of C-terminal carboxylates shown in Scheme II is somewhat analogous to known hydrolysis reactions in which a neutral carboxylate -OH oxygen is involved in intramolecular nucleophilic attack on an amide or other carbonyl carbon.<sup>15</sup> In contrast to the carboxylate chemistry, however, esters<sup>16</sup> and amides<sup>16d,17</sup> inherently do not undergo this same type of intramolecular reaction because the most nucleophilic site in esters is not the methoxy oxygen, and in amides, it is not the amide nitrogen. Instead, the most nucleophilic site in both esters and amides is the carbonyl oxygen. Thus, the two latter moieties undergo nucleophilic attack via an entirely different transition state from that of the carboxylates.<sup>16,17</sup>

**Formation of Other Product Ions.** We previously<sup>12</sup> addressed formation of N-terminal  $(a_{n-m} + \text{Cat} - \text{H})^+$  and C-terminal  $(y_{n-m} + \text{Cat} + \text{H})^+$  product ions (Figures 1 and 2). We also<sup>12</sup> presented evidence that they likewise arise from  $(\text{M} + \text{Cat})^+$  complexes that contain the alkali metal ion bonded to a neutral peptide molecule. There is another small and generally weakly abundant ion series, the N-terminal  $(b_{n-m} + \text{Cat} - \text{H})^+$  product ions, usually represented by at most a  $(b_n + \text{Cat} - \text{H})^+$  and a  $(b_{n-1} + \text{Cat} - \text{H})^+$  ion. The  $(b_n + \text{Cat} - \text{H})^+$  ion, if it is present, arises by loss of  $\text{H}_2\text{O}$ ,  $\text{NH}_3$ , or  $\text{CH}_3\text{OH}$  from C-terminal acids, amides, and methyl esters, respectively. The  $(b_{n-1} + \text{Cat} - \text{H})^+$  ion results from cleavage of the amide OC-NH bond between the C-terminal and adjacent amino acid (" $b_3$ " in Figure 2A,B). Formation of both product ions requires transfer of hydrogen to a neutral leaving group.

It is difficult to address the mechanism for formation of these ions because of their scarcity in the CID spectra. We find, however, that neither converting the C-terminal amino acid into an ester nor N-acetylation and esterification stops formation of  $(b_{n-m} + \text{Cat} - \text{H})^+$  ions. Furthermore, from structural changes in the peptides,<sup>18</sup> neither Pro nor Gly as the  $n-m$  amino acid stops

(15) (a) Menger, F. M.; Ladika, M. *J. Am. Chem. Soc.* **1988**, *110*, 6794-6796. (b) Bender, M. L.; Chow, Y.-L.; Chloupek, J. *J. Am. Chem. Soc.* **1958**, *80*, 5380-5384. (c) Bender, M. L. *J. Am. Chem. Soc.* **1957**, *79*, 1258-1259. (d) Leach, S. J.; Lindley, H. *Trans. Faraday Soc.* **1953**, *49*, 921-925.

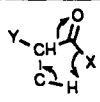
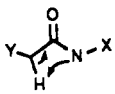
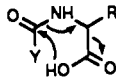
(16) (a) Singh, A.; Andrews, L. J.; Keefer, R. M. *J. Am. Chem. Soc.* **1962**, *84*, 1179-1185. (b) Lovins, R. E.; Andrews, L. J.; Keefer, R. M. *J. Am. Chem. Soc.* **1962**, *84*, 3959-3962. (c) Andrews, L. J.; Keefer, R. J. *J. Am. Chem. Soc.* **1959**, *81*, 4218-4223. (d) Keefer, R. M.; Andrews, L. J. *J. Am. Chem. Soc.* **1959**, *81*, 5329-5333.

(17) (a) Lawson, W. B.; Gross, E.; Foltz C. M.; Witkop, B. *J. Am. Chem. Soc.* **1962**, *84*, 1715-1718. (b) Stirling, C. J. M. *J. Chem. Soc.* **1960**, 252-262.

(18) Although neither deuterium-labeling nor MS-MS-MS experiments were used to evaluate this reaction mechanism, we previously used this same approach in our studies of peptide-alkali<sup>12</sup> and peptide-alkaline earth<sup>13</sup> metal ion complexes. This approach assumes that the drastic effects of structural changes that form the basis for our conclusions are not simple substituent effects.

(14) (a) Berthod, H.; Pullman, A. *J. Comput. Chem.* **1981**, *2*, 87-95. (b) Gresh, N.; Pullman, A.; Claverie, P. *Int. J. Quantum Chem.* **1985**, *28*, 757-771.

**Table I.** Summary of Proposed Mechanisms for Fragmentation of Peptide (M + Cat)<sup>+</sup> Complexes

	$(a_{n-m} + \text{Cat} - \text{H})^+$	$(y_{n-m} + \text{Cat} + \text{H})^+$	$(b_{n-m} + \text{Cat} + \text{OH})^+$
proposed transition state <sup>a</sup>			
thermal analogy	acyl chlorides <sup>22</sup>	<i>tert</i> -butylamine <sup>19</sup>	
$E_0$ (kcal mol <sup>-1</sup> )	50–55	67	
Arrhenius $A$ factor (s <sup>-1</sup> )	$\sim 10^{13}$ – $10^{14}$	$\sim 10^{14}$	
location of metal ion	toward N-terminus	toward C-terminus	toward N-terminus

<sup>a</sup>See ref 12 for details of proposed mechanisms for  $(a_{n-m} + \text{Cat} - \text{H})^+$  and  $(y_{n-m} + \text{Cat} + \text{H})^+$  product ions.

formation of these product ions. These data suggest that hydrogen is transferred from the  $\alpha$ -carbon of the  $n$ - $m$  amino acid, perhaps via the mechanism shown in Scheme IV in which X = OH, NH<sub>2</sub>, OCH<sub>3</sub>, or NH-CHR-COX, and Y = NH<sub>2</sub>, C<sub>6</sub>H<sub>5</sub>CONH, or CH<sub>3</sub>CONH. This possible mechanism involves a four-membered transition state that is somewhat analogous to the thermolytic 1,2-elimination of NH<sub>3</sub> and isobutene from *tert*-butylamine, which has an activation energy of 67 kcal mol<sup>-1</sup> and an Arrhenius  $A$  factor of  $\sim 10^{14}$  s<sup>-1</sup>.<sup>19</sup> The transition state is identical with one that we proposed for formation of C-terminal  $y$ -sequence ions from complexes that contain either alkaline earth<sup>13</sup> or alkali<sup>12</sup> metal ions. Here, however, the metal ion would be located on the N-terminal side of the cleavage reaction instead of on the C-terminal side, the latter which characterizes formation of  $y$ -sequence ions.<sup>12</sup> The exact location of the alkali metal ion is unknown, but the favored gas-phase Li ion binding sites in a simple peptide would be at amide oxygens ( $-\Delta G_{\text{Li}}$  for HCONHMe = 42.4 kcal mol<sup>-1</sup>)<sup>14</sup> and not at the N-terminal amine ( $-\Delta G_{\text{Li}}$  for MeNH<sub>2</sub> = 34.9 kcal mol<sup>-1</sup>).<sup>1b,4,3b,c</sup>

Grese, Cerny, and Gross<sup>10a</sup> were the first to address formation of  $(b_{n-1} + \text{Cat} - \text{H})^+$  ions, specifically in relation to peptides that contain Arg as the second amino acid from the C-terminus. Their mechanism involves (M + Cat)<sup>+</sup> complexes that first undergo the reaction of Scheme I to give  $(b_{n-1} + \text{Cat} + \text{OH})^+$  ions, and then these product ions subsequently undergo loss of H<sub>2</sub>O from the Arg residue to give the final  $(b_{n-1} + \text{Cat} - \text{H})^+$  ions. Our results discussed above regarding formation of  $(b_{n-m} + \text{Cat} + \text{OH})^+$  ions do not support such a mechanism. Furthermore, we find that (M + Cat)<sup>+</sup> complexes of the C-terminal ester of Gly-Pro-Arg-Pro still decompose to give  $(b_{n-1} + \text{Cat} - \text{H})^+$  ions even though no  $(b_{n-1} + \text{Cat} + \text{OH})^+$  ions can be formed.<sup>20</sup> As seen in some MS<sup>3</sup> experiments, however, the  $(b_{n-1} + \text{Cat} + \text{OH})^+$  ions can decompose by loss of H<sub>2</sub>O to give the  $(b_{n-1} + \text{Cat} - \text{H})^+$  product ion, but this loss can be described by the reaction in Scheme IV.<sup>21</sup>

#### Relative Ion Abundances vs Location of Alkali Metal Ion.

Previous researchers tried to relate relative product ion abundances in metastable ion and CID spectra of peptide (M + Cat)<sup>+</sup> complexes to gas-phase equilibrium alkali metal ion or proton affinities.<sup>7,10b</sup> Such relationships could exist if significantly different equilibrium populations of isomeric (M + Cat)<sup>+</sup> complexes, which contained the metal ion bonded in a different location, were fragmenting at the same rates and thus via the same transition state. It is clear, however, from the mechanisms in Schemes II–IV and in Table I, that transition states for each of the different types of reactions are significantly different. Alternately, such relationships could exist for one population of decomposing (M + Cat)<sup>+</sup> ions if the rates of the different competing fragmentation reactions, and thus individual activation energies and transition-state geometries, reflected the thermodynamic equilibria. The

**Table II.** Absolute Abundances (%) of  $(b_{n-1} + \text{Na} + \text{OH})^+$  and  $(a_{n-m} + \text{Na} - \text{H})^+$  Product Ions in Metastable Ion and CID Spectra<sup>a</sup>

precursor	product ion	metastable	CID	% increase <sup>b</sup>
$(\text{VAAF} + \text{Na})^+$	$b_3$	0.88	2.7	207
	$a_3$	0.009	0.19	2011
$(\text{YGGFL} + \text{Na})^+$	$b_4$	3.6	3.8	5.6
	$a_4$	0.18	0.69	283
$(\text{RVYVHPF} + \text{Na})^+$	$b_6$	0.21	0.27	29
	$a_5$	0.15	0.60	300

<sup>a</sup>The absolute abundances are expressed as % relative to the main beam not including loss of the alkali cation as Na<sup>+</sup>, which is not observable in the B/E scans. <sup>b</sup>This is the percent increase in ion abundances as a result of CID.

difficulty here with such a concept is that, again, the transition states for the different reactions are significantly different (Table I) and would not be inherently expected to reflect thermodynamic equilibria. Furthermore, the relative rates of the different reactions will not only depend upon the specific transition state but will also reflect from subtle to significant effects that result from metal ion binding. For example, as we discussed previously in relation to binding between alkaline earth metal ions and peptides,<sup>13</sup> a reduction in reaction rate and thus product ion formation could result from metal ion complexation that prevents attainment of a particular transition state. Conversely, an increase in reaction rate and formation of a product ion could result from a metal ion interaction that specifically polarizes the bonds that are involved in the transition state. We also showed previously<sup>12</sup> that there is no simple relationship between product ion abundances in CID spectra of different peptide (M + Cat)<sup>+</sup> complexes and either equilibrium proton or lithium ion affinities of the constituent amino acids. In addition, a comparison of spectra A and B in Figure 2 shows that relative ion abundances in the CID spectra may be dependent upon experimental conditions, three of which are field-free region, collision gas pressure, and center-of-mass energy.

In spite of these limitations, it is possible to use changes in fragment ion abundances between metastable ion and CID spectra to address relative rates of different decomposition reactions. Changes in reaction rates with changes in peptide structure may provide information regarding effects of metal ion binding on transition-state energies. Such an idea was originally used by Gross and co-workers<sup>10a</sup> to provide support for the mechanism in Scheme I. For example, metastable ion spectra of (M + Na)<sup>+</sup> complexes of peptides that contain alkyl side chains generally show virtually no  $(a_{n-1} + \text{Na} - \text{H})^+$  ions, although  $(b_{n-1} + \text{Na} + \text{OH})^+$  ions are highly abundant ( $n - 1 = 3$  in Figure 3A). The  $(a_{n-1} + \text{Na} - \text{H})^+$  ions can be clearly observed, however, in the corresponding CID spectrum ( $a_3$  ions in Figure 3D). In peptides that contain phenyl side chains,  $(a_{n-1} + \text{Na} - \text{H})^+$  ions can be detected in both metastable ion ( $a_4$  ions in Figure 3B) and CID spectra (Figure 3E), although they become significantly more abundant in the latter. For peptides that contain histidine as either the  $n - 1$  or  $n - 2$  amino acid,  $(a_{n-1/n-2} + \text{Na} - \text{H})^+$  ions generally are even more easily detected in metastable ion spectra ( $a_5$  ions in Figure 3C), and they increase in CID spectra sometimes to the extent of overwhelming the  $(b_{n-1} + \text{Na} + \text{OH})^+$  ions (Figure 3F).

The changes in relative abundances of the  $(b_3 + \text{Na} + \text{OH})^+$  vs the  $(a_3 + \text{Na} - \text{H})^+$  ions in the benchmark example of peptides that contain alkyl chains (Figure 3, A and D) provide immediate information regarding the kinetics of the two reactions: The  $(a_3$

(19) Robinson, P. J.; Halbrook, K. A. *Unimolecular Reactions*; Wiley-Interscience: London, 1972; pp 231–236.

(20) The N-terminal  $(b_3 + \text{Na} - \text{H})^+$  product ions are observed in CID spectra of (GPRP + Na)<sup>+</sup> and (N-acetyl-GPRP-OCH<sub>3</sub> + Na)<sup>+</sup> in absolute abundances of 4.4 and 0.08%, respectively. The latter absolute abundance is weaker because new fragment ions, which appear to be internal fragments, become significantly abundant for the derivatized peptide.

(21) One MS<sup>3</sup> experiment shows that the  $(b_4 + \text{Na} + \text{OH})^+$  ions from (M + Na)<sup>+</sup> complexes of YGGFLK undergo subsequent loss of H<sub>2</sub>O.

(22) (a) Lennon, B. S.; Stimson, V. R. *J. Am. Chem. Soc.* **1969**, *91*, 7562–7564. (b) Lennon, B. S.; Stimson, V. R. *Aust. J. Chem.* **1970**, *23*, 525–531.

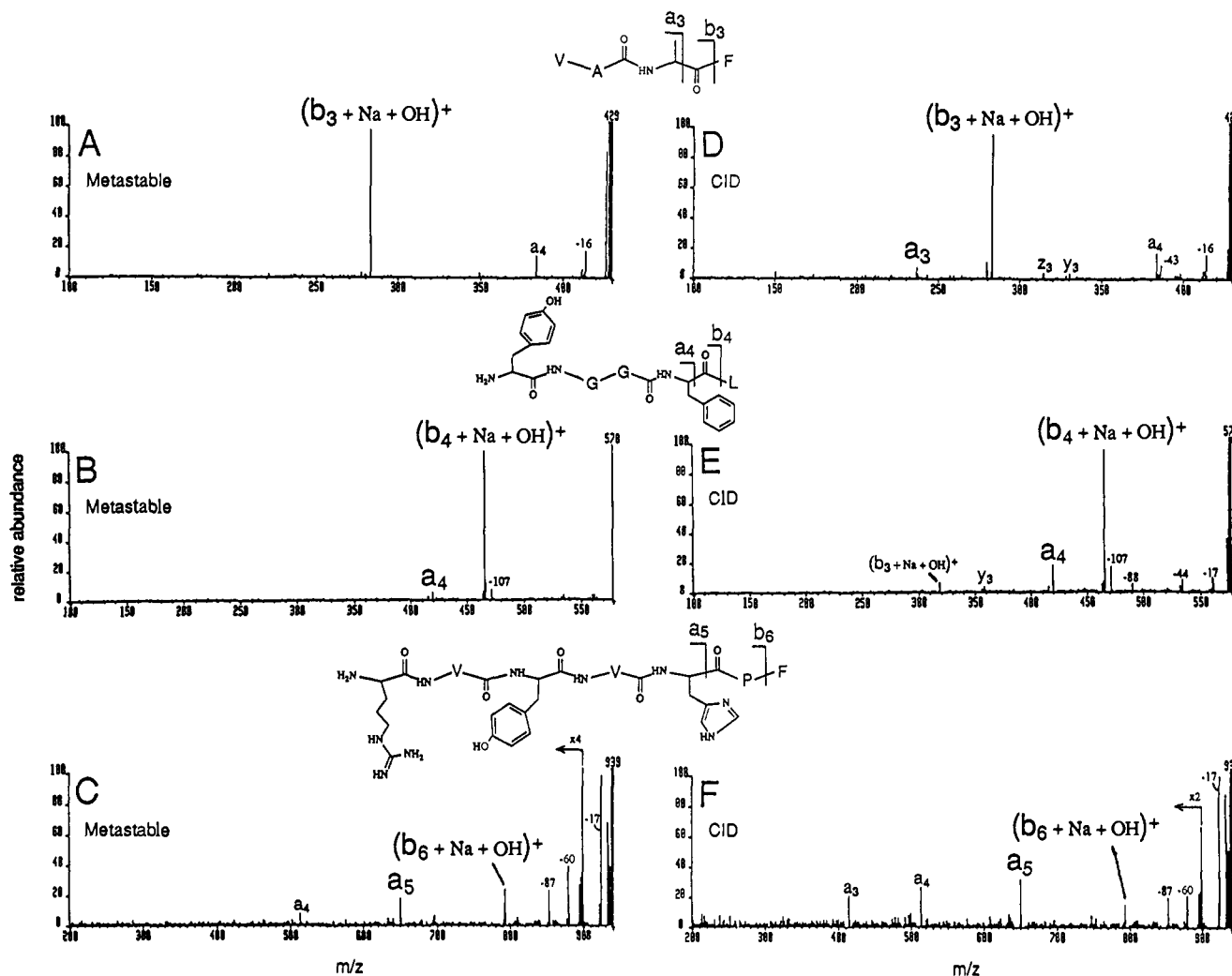


**Figure 3.** Metastable ion and CID spectra of  $(M + Na)^+$  complexes of (A and D) Val-Ala-Ala-Phe; (B and E) Tyr-Gly-Gly-Phe-Leu; and (C and F) Arg-Val-Tyr-Val-His-Pro-Phe, respectively, acquired by using the VG 70-s (at Emory). Ions labeled  $a_{n-m}$ ,  $b_{n-m}$ ,  $y_{n-m}$ , and  $z_{n-m}$  are  $(a_{n-m} + Na - H)^+$ ,  $(b_{n-m} + Na - H)^+$ ,  $(y_{n-m} + Na + H)^+$ , and  $(z_{n-m} + Na)^+$  ions, respectively.

$+ Na - H)^+$  ions must arise from a higher energy or faster reaction than the  $(b_3 + Na + OH)^+$  ions because they are virtually absent in the metastable ion spectrum (Figure 3A,  $\log k(E) \sim 6 \text{ s}^{-1}$ , in which  $E =$  precursor ion internal energy) but are clearly detectable in the CID spectrum (Figure 3D,  $\log k(E) \geq 6 \text{ s}^{-1}$ ). These kinetics are further supported from changes in absolute abundances of  $(b_{n-1} + Na + OH)^+$  vs  $(a_{n-m} + Na - H)^+$  ions between metastable ion and CID spectra (Table II): For each peptide, the percent increase in absolute abundances of  $(a_{n-m} + Na - H)^+$  ions as a result of collisional activation is from 10 to 50 times the percent increase in abundances of  $(b_{n-1} + Na + OH)^+$  ions. Data in both Figure 3 and Table II indicate, however, that formation of  $(b_{n-1} + Na + OH)^+$  ions becomes decreasingly competitive in both the metastable ion and CID time frames as the side chains become increasingly more capable of interacting with the alkali metal ion. This is most apparent in comparing the data in Table II for YGGFL (Figure 3 B and E) to the data for RVYVHPF (Figure 3, C and F). That is, in both the metastable ion and CID time frames for these two peptide complexes, the absolute abundances of the YGGFL  $a_4$  vs RVYVHPF  $a_5$  ions change little with the changing side-chain structure, but absolute abundances of  $(b_{n-1} + Na + OH)^+$  ions decrease by  $\sim 90\%$  in changing from YGGFL to RVYVHPF. Thus, rates of reactions that give  $(b_{n-1} + Na + OH)^+$  ions appear more sensitive to structural changes than rates of reactions that give  $(a_{n-m} + Na - H)^+$  ions.

These data suggest the following: (1) threshold energies for reactions that give  $(b_{n-1} + Na + OH)^+$  ions are less than those for reactions that give  $(a_{n-m} + Na - H)^+$  ions; and (2) long  $k(E)$  vs  $E$  curves for  $(b_{n-1} + Na + OH)^+$  ions are less steeply sloped

than curves for  $a_{n-m}$  ions. A third conclusion is that threshold energies for reactions that give  $(b_{n-1} + Na + OH)^+$  ions increase with increasing chelating ability of the side chains, whereas threshold energies for reactions that give  $(a_{n-m} + Na - H)^+$  ions remain relatively constant. These ideas are summarized by the hypothetical  $\log k(E)$  vs  $E$  curves shown in Figure 4A,B. The curves in Figure 4A have been drawn to schematically reflect abundances of  $(a_4 + Na - H)^+$  and  $(b_4 + Na + OH)^+$  ions in Figure 3, B and E, whereas those in Figure 4B are meant to reflect abundances of  $(a_5 + Na - H)^+$  and  $(b_6 + Na + OH)^+$  ions in Figure 3, C and F. The schematic in Figure 4 also can be extrapolated, by shifting  $E_{\alpha(b)}$  to an even lower value, to explain the ion abundances in spectra in Figure 3, A and D, for a nonbonding side chain. (A more accurate representation of relative ion abundances would require convoluting  $P(E)$  with the  $\log k(E)$  curves suggested in Figure 4.)

Changes in the threshold energies for formation of  $(b_{n-1} + Cat + OH)^+$  ions can be understood from differences in how the metal ion is bonded by the side chains in the fragmenting  $(M + Cat)^+$  complexes. The mechanism for formation of  $(b_{n-1} + Cat + OH)^+$  product ions in Scheme II is shown to require the alkali metal ion to be directly bonded to the oxygen of the C-terminal amide that is being attacked by the carboxylate  $-OH$ . (In contrast, formation of  $(a_{n-1} + Cat - H)^+$  ions instead requires the metal ion to be bonded on the *second* or greater amide oxygen from the C-terminus.<sup>12</sup>) The structural requirement for formation of  $(b_{n-1} + Cat + OH)^+$  product ions is supported by the experimental observation that formation of these ions becomes less competitive for complexes that contain the larger<sup>23</sup> and more polarizable<sup>24</sup>

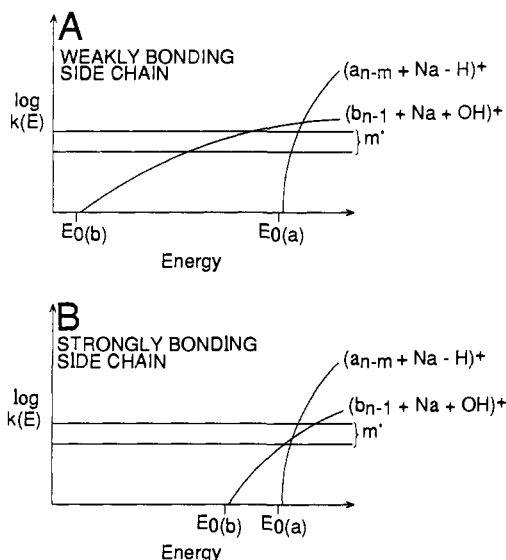


**Figure 4.** Schematic  $\log k(E)$  vs  $E$  curves for formation of  $(a_{n-m} + \text{Cat} - \text{H})^+$  and  $(b_{n-1} + \text{Cat} + \text{OH})^+$  product ions from peptide complexes that contain (A) weakly bonding side chains (refer to Figure 3, B and E) and (B) strongly bonding side chains (refer to Figure 3, C and F). The horizontal band represents the range of rate constants that lead to metastable ion ("m") reactions in the first field-free region of the VG 70-S.

$\text{K}^+$  and  $\text{Rb}^+$ , and virtually stops for  $\text{Cs}^+$ .<sup>12</sup> From this, we conclude that metal ion binding to the C-terminal amide oxygen, and the resulting increased electrophilicity of the carbonyl carbon,<sup>3d,25</sup> is the primary driving force for the reaction. Thus, a stronger and more specific interaction between the metal ion and a chelating side chain that results in a weakening of the metal ion bond to the C-terminal amide would increase the threshold energy for formation of  $(b_{n-1} + \text{Cat} + \text{OH})^+$  product ions, shift the  $\log k(E)$  vs  $E$  curve to higher energies, and decrease product ion formation in both the metastable ion and CID time frames. Such specific interactions would occur for side chains that can bond more strongly to the metal ion to form a more stable chelate structure. Such side chains are ones that contain phenyl rings (Phe and Tyr, Figure 3, B and E) and especially ones that contain imidazole (His) and guanidine (Arg) (Figure 3, C and F). Thus, the thermodynamics (i.e., stability) of a metal ion binding interaction in the  $(\text{M} + \text{Cat})^+$  complexes can affect the rates of different reactions, and thus different product ion abundances, by changing the transition-state energy for the  $(b_{n-1} + \text{Cat} + \text{OH})^+$  product ions relative to others.

The evidence presented in Figures 3 and 4 and Table II supports decompositions of  $(\text{M} + \text{Cat})^+$  complexes that exist as multidentate, chelated structures in which the alkali metal ion is intramolecularly bonded to several sites in the peptide.<sup>26</sup> Our proposal is also supported by our previous<sup>12</sup> results that showed marked changes in fragmentation patterns with increasing size of alkali metal ion, results consistent with multidentate interactions between the metal ion and the peptide. Decomposition of multidentate  $(\text{M} + \text{Cat})^+$  complexes also can explain the successive formation of  $(b_{n-m} + \text{Cat} + \text{OH})^+$  and  $(b_{n-m} + \text{Cat} + \text{OH} - 88)^+$  ions from the peptides considered in this paper (given in Figure

2 and in ref 27). That is, step-wise formation of successively smaller mass ions via the reactions in Schemes II and III can be envisioned as requiring the alkali metal ion to be bonded to the  $n-1$ ,  $n-2$ ,  $n-3$ , and  $n-4$  amide carbonyls of HLGLAR (Figure 2). This mechanism is supported by theoretical calculations by Rode and Honnongbua<sup>28</sup> and by Leary et al.<sup>11b</sup> that indicate that structures in which the alkali metal ion is coordinated to several chelating functional groups are significantly more stable than structures in which the metal is bonded to a single site. It is unfortunate that Leary et al.<sup>11b</sup> did not investigate the exact type of structure shown in Scheme II so that we could have an idea of its stability relative to other intramolecularly bonded species.

## Conclusions

Evidence is presented here for the mechanism for formation of N-terminal  $(b_{n-m} + \text{Cat} + \text{OH})^+$  product ions from  $(\text{M} + \text{Cat})^+$  complexes between peptides and alkali metal ions. The intramolecular nucleophilic reaction first proposed by Westmore and co-workers<sup>8</sup> explains both our and previous<sup>9-11</sup> experimental results. This mechanism may also explain recent results of Gaskell and co-workers<sup>29</sup> in which an analogous fragmentation is shown to occur for  $(\text{M} + \text{H})^+$  ions of peptides. Furthermore, a 1,2-elimination reaction can describe formation of  $(b_{n-m} + \text{Cat} - \text{H})^+$  product ions. Both types of N-terminal  $b$ -product ions arise from  $(\text{M} + \text{Cat})^+$  complexes that contain the metal ion bonded on the N-terminal side of the site of reaction. Kinetic results from metastable ion and CID experiments support multidentate bonding of the alkali metal ion to several sites in the peptide molecule, and these can include basic amide oxygens and chelating side chains. We showed previously<sup>12</sup> that there are no simple relationships between basicities of amino acid side chains and fragmentation patterns. The presence of a basic side chain is important in the binding interactions, nonetheless, as demonstrated in Figures 2A and 3F that show more detailed sequences of fragment ions for His- and Arg-containing peptides than are shown in Figures 1 and 3D,E for the other peptides.

Our experimental results here and in a previous paper<sup>12</sup> thus do not support fragmentations of gas-phase  $(\text{M} + \text{Cat})^+$  complexes that contain the alkali metal ion bonded to a deprotonated carboxylate anion.<sup>9-11</sup> Consequently, the fragmentations do not reflect solution-phase binding to a peptide zwitterion, but instead they do reflect binding to intrinsically basic sites in a neutral peptide molecule. Furthermore, formation of multidentate  $(\text{M} + \text{Cat})^+$  complexes is analogous to the types of intramolecular binding interactions that occur between alkali metal ions and less hydrophilic binding centers in enzymes.<sup>30</sup>

## Experimental Section

Peptides were obtained either from Sigma or from the Emory University Microchemistry Center. Standard techniques<sup>31</sup> were used to prepare C-terminal methyl esters and other derivatives. The peptides included RVYVHPF; YGGFLK, HLGLAR; RYLPT, VHLTP, YPFPG, YGGFM, FFFFF, *t*-Boc-YAG[N-Me]FG-ol, YGGFL, YGGFL-NH<sub>2</sub>, FLEEI, and FLEEL; ALAL, ALAL-OCH<sub>3</sub>, FFFF, GPRP, *N*-acetyl-GPRP-OCH<sub>3</sub>, GPGG, VAAF, VAAF-OCH<sub>3</sub>, AGFL, GGFL, AGFM, GGFM, GGFM-NH<sub>2</sub>, and *N*-acetyl-GGFM-OCH<sub>3</sub>; ALG, GLY, MLF, GLF, GGV, GGV-OCH<sub>3</sub>, FFF, IPI, *N*-benzoyl-GGG, *N*-benzoyl-GHL, *p*-OH-*N*-benzoyl-GHL, and AAA-OCH<sub>3</sub>; AL, IN, LG, LG-OCH<sub>3</sub>, FF, LL, LL-OCH<sub>3</sub>, GH, *N*-benzoyl-GK, *N*-benzoyl-GF, and GL-NH<sub>2</sub>; and permethylated *N*-benzoyl-GF, *N*-acetyl-LG, *N*-acetyl-GGV, *N*-acetyl-YGGFL-NH<sub>2</sub>, and *N*-acetyl-GGFM-NH<sub>2</sub>.

(23) Morris, D. F. C. In *Structure and Bonding*; Jørgensen, C. K., Neilands, J. B., Nyholm, R. S., Reinen, D., Williams, R. J. P., eds.; Springer-Verlag: New York, 1968; vol. 4, pp 63-82.

(24) Eliezer, I.; Krindel, P. *J. Chem. Phys.* **1972**, *57*, 1884-1891.

(25) (a) Rode, B. M.; Breuss, M.; Schuster, P. *Chem. Phys. Lett.* **1975**, *32*, 34-37. (b) Miaskiewicz, K.; Sadlej, J. *J. Molec. Struct. (Theochem)* **1985**, *124*, 223-230. (c) Rode, B. M.; Preuss, H. *Theor. Chim. Acta (Berl.)* **1974**, *35*, 369-378.

(26) For example, if the  $(a_{n-m} + \text{Cat} - \text{H})^+$  product ions arose from precursor complexes that were structurally different from, and preferentially formed over, those that gave  $(b_{n-1} + \text{Cat} + \text{OH})^+$  ions, we would expect the absolute, and relative, abundances of the  $(a_{n-m} + \text{Cat} - \text{H})^+$  ions to increase in going from YGGFL to RVYVHPF. This, however, is not observed experimentally (Table II).

(27) Successive losses to give  $(b_{n-m} + \text{Cat} + \text{OH})^+$  ions also can be seen in the CID spectrum of  $(\text{M} + \text{Na})^+$  complexes of YGGFLK, which shows a series of  $b_5$ ,  $b_4$ , and  $b_3$  ions. Furthermore, MS<sup>3</sup> experiments shows that the  $(b_5 + \text{Na} + \text{OH})^+$  ions decompose to give both the  $b_4$  and  $b_3$  ions; the  $(b_4 + \text{Na} + \text{OH})^+$  ions also decompose to give the  $b_3$  ions. Peptides that give successive losses of 88 u were discussed earlier in the text.

(28) Rode, B. M.; Honnongbua, S. V. *Inorg. Chim. Acta* **1985**, *96*, 91-97. (29) Thorne, G. C.; Ballard, K. D.; Gaskell, S. J. *J. Am. Soc. Mass Spectrom.* **1990**, *1*, 249-257.

(30) (a) Pressman, B. C. In *Inorganic Biochemistry*; Eichhorn, G. L., ed.; Elsevier Scientific: Amsterdam, 1973; pp 203-226. (b) Williams, R. J. P. *Adv. Chem. Ser.* **1971**, *100*, 155-173.

(31) Knapp, D. A. *Handbook of Analytical Derivatization Reactions*; Wiley: New York, 1979; pp 249-253, 327-335.



Matrices used for fast atom bombardment (FAB) were 3-nitrobenzyl alcohol, 5:1 dithiothreitol/dithioerythreitol, and 2:1 thioglycerol/glycerol and were obtained from Aldrich. The  $(M + \text{Cat})^+$  complexes were prepared by mixing small amounts ( $\mu\text{g}$ ) of the peptides with one of the FAB matrices, which had been previously saturated with an alkali iodide.

Most mass spectrometric experiments were performed by using a VG 70-S, forward-geometry (EB, in which E = ESA and B = magnet) mass spectrometer (at Emory). The VG 70-S is equipped with an Ion Tech saddle-field FAB gun and a commercial FAB ion source. Precursor ions were produced by bombarding the sample with 7-keV Ar atoms at an atom gun current of 2 mA and were accelerated to 8-keV translational energy. Product ions that were formed metastably or by collision with He (analyzer pressure of  $1 \times 10^{-6}$  Torr;  $\sim 50\%$  beam reduction) in the first field-free region between the ion source and the ESA were observed by using B/E scans. Experiments were performed at a product ion resolution of approximately 1000 (10% valley), and magnet calibration was performed by using a mixture of LiI, NaI, RbI, and CsI in  $\text{H}_2\text{O}$ . All spectra were acquired by using VG software, and metastable ion and CID spectra are the result of averaging between 10 and 20 scans. Background spectra were acquired for all experiments in order to eliminate artifact product ions that might arise from chemical noise.<sup>44</sup>

The MS-MS and MS-MS-MS ( $\text{MS}^3$ ) experiments involved using a JEOL HX110/HX110, tandem, four-sector ( $\text{EB}_1$ - $\text{EB}_2$ ) mass spectrometer (at the Structural Biochemistry Center, University of Maryland Baltimore County, or UMBC). Precursor ions were produced by using a JEOL FAB gun and 6-keV Xe atoms. Here, all CID spectra were acquired at 10-kV accelerating voltage by using He at 70% beam reduction. The MS-MS experiments were performed by using  $\text{EB}_1$  to energy and mass select the  $(M + \text{Cat})^+$  complexes, which were then collided with He in a collision cell in the third field-free region. A linked scan of  $\text{EB}_2$  was used to obtain spectra of the first-generation product ions. The  $\text{MS}^3$  experiments were performed by colliding the  $(M + \text{Cat})^+$  complexes with He in the first field-free region between the FAB ion source and  $\text{EB}_1$  and then using  $\text{EB}_1$  to energy and mass select first-generation product ions. The selected first-generation ("intermediate") product ions were then collided with He in the third field-free region between  $\text{EB}_1$  and  $\text{EB}_2$ . A linked scan of  $\text{EB}_2$  was then used to obtain a

spectrum of the second-generation product ions. Resolution was approximately 1000 for both  $\text{EB}_1$  and  $\text{EB}_2$ , and  $\text{MS}^3$  spectra are the result of an averaging between 2 and 10 scans.

**Acknowledgment.** The Emory University Research Fund and the donors of the Petroleum Research Fund, administered by the American Chemical Society, provided partial support for this research. Recognition is made to the NIH for the use of the VG 70-S, a shared instrument, and to the NSF for the use of the JEOL HX110/HX110 at the Structural Biochemistry Center at the University of Maryland Baltimore County, an NSF supported Biological Instrumentation Center. A preliminary report of these results was presented at the 38th ASMS Conference on Mass Spectrometry and Allied Topics, June 1990, Tucson, Arizona.

**Registry No.** RYVYVHPF, 16376-83-3; YGGFLK, 83404-43-7; HLGLAR, 66157-45-7; RYLPT, 57966-42-4; VHLTP, 93913-38-3; YPFPF, 72122-63-5; YGGFM, 58569-55-4; FFFFF, 65757-10-0; BOC-YAG[N-Me]FG-01, 126616-16-8; YGGFL, 58822-25-6; YGGFL-NH<sub>2</sub>, 60117-24-0; FLEEI, 62733-72-6; FLEEL, 69729-06-2; ALAL, 84676-48-2; ALAL-OMe, 131131-84-5; FFFF, 2667-02-9; GPRP, 67869-62-9; Ac-GPRP-OMe, 132884-57-2; GPGG, 13054-03-0; VAAF, 21957-32-4; VAAF-OMe, 131131-85-6; AGFL, 119530-65-3; GGFL, 60254-83-3; AGFM, 126616-17-9; GGFM, 61370-88-5; GGFM-NH<sub>2</sub>, 84969-59-5; Ac-GGFM-OMe, 132884-58-3; ALG, 60030-20-8; GLY, 4306-24-5; MLF, 59881-08-2; GLF, 103213-38-3; GGV, 20274-89-9; GGV-OMe, 66328-83-4; FFF, 2578-81-6; IPI, 90614-48-5; PhCO-GGG, 31384-90-4; PhCO-GHL, 31373-65-6; 4-HOC<sub>6</sub>H<sub>4</sub>CO-GHL, 77697-23-5; AAA-OMe, 30802-27-8; AL, 3303-34-2; IN, 59652-59-4; LG, 686-50-0; LG-OMe, 27560-15-2; FF, 2577-40-4; LL, 3303-31-9; LL-OMe, 13022-42-9; GH, 2489-13-6; PhCO-GK, 740-63-6; PhCO-GF, 744-59-2; GL-NH<sub>2</sub>, 17331-92-9; PhCO-[N-Me]G[N-Me]F-OMe, 132884-59-4; Ac-LG, 4033-42-5; Ac-GGV, 97530-33-1; Ac-YGGFL-NH<sub>2</sub>, 132910-39-5; Ac-GGFM-NH<sub>2</sub>, 132884-60-7; LiI, 10377-51-2; NaI, 7681-82-5; KI, 7681-11-0; RbI, 7790-29-6; CsI, 7789-17-5.

## Migratory Insertion of Ethylene into Iron-Hydrogen Bonds and $\beta$ -Hydride Elimination of Ethyl Groups on H-Covered Fe(100)

M. L. Burke<sup>†</sup> and R. J. Madix<sup>\*‡</sup>

*Contribution from the Department of Chemistry and the Department of Chemistry and Chemical Engineering, Stanford University, Stanford, California 94305. Received October 22, 1990. Revised Manuscript Received January 14, 1991*

**Abstract:** Ethylene has been found to adsorb reversibly at 110 K without dissociation on Fe(100) presaturated with hydrogen. No ethane is formed following adsorption of ethylene, nor does any ethylene decompose on this surface. Desorption of ethylene at 160 K competes with the formation of adsorbed ethyl groups. Ethyl groups decompose by  $\beta$ -hydride elimination with an activation barrier of  $12.2 \pm 0.6$  kcal/mol and a preexponential factor of  $10^{13.4 \pm 0.6} \text{ s}^{-1}$ , exhibiting a primary kinetic isotope effect,  $k_{\text{H}}/k_{\text{D}}$ , at 219 K of  $4.9 \pm 0.5$ . The reversible reaction of adsorbed ethylene and adsorbed deuterium to form ethyl groups leads to the incorporation of up to four D atoms in the ethylene evolved during temperature-programmed reaction. The activation energies determined here indicate that barriers to formation and  $\beta$ -hydride elimination of adsorbed ethyl groups agree with those observed for transition-metal complexes only after the energetics of structural rearrangements in the complex are removed.

### 1. Introduction

Over the last 10 years there has been considerable interest in the "cluster-surface analogy".<sup>1-3</sup> In order to contribute to the general understanding of transition-metal chemistry in all of its regimes, we have undertaken surface studies of one of the most

fundamental and well-studied homogeneous catalytic reactions, olefin hydrogenation. In the present study we have directed our efforts toward the elucidation of the fundamental kinetic and mechanistic aspects of ethylene hydrogenation on an iron surface.

\* Author to whom correspondence should be addressed.

<sup>†</sup> Department of Chemistry.

<sup>‡</sup> Department of Chemistry and Chemical Engineering.

(1) Muetterties, E. L. *Bull. Soc. Chim. Belg.* **1975**, *84*, 959.

(2) Muetterties, E. L.; Rhodin, T. N.; Band, E.; Brucker, C. F.; Pretzer, W. R. *Chem. Rev.* **1979**, *79*, 91.

(3) Canning, J.; Madix, R. J. *J. Phys. Chem.* **1984**, *88*, 2437.